Ruthenium^{II}(*p*-cymene) complexes bearing ligands of the type 1-[2'-(methoxycarbonyl)phenyl]-3-[4'-X-phenyl]triazenide (X= F, Cl, Br, I): synthesis, structure and catalytic activity

Erick Correa-Ayala, Carlos Campos-Alvarado, Daniel Chávez, David Morales-Morales, Simón Hernández-Ortega, Juventino J. García, Marcos Flores-Álamo, Valentín Miranda-Soto, Miguel Parra-Hake

PII: S0020-1693(17)30673-4
DOI: http://dx.doi.org/10.1016/j.ica.2017.06.064
Reference: ICA 17713

To appear in: *Inorganica Chimica Acta*

Received Date: 4 May 2017
Revised Date: 23 June 2017
Accepted Date: 28 June 2017

Please cite this article as: E. Correa-Ayala, C. Campos-Alvarado, D. Chávez, D. Morales-Morales, S. Hernández-Ortega, J.J. García, M. Flores-Álamo, V. Miranda-Soto, M. Parra-Hake, Ruthenium^{II}(*p*-cymene) complexes bearing ligands of the type 1-[2'-(methoxycarbonyl)phenyl]-3-[4'-X-phenyl]triazenide (X= F, Cl, Br, I): synthesis, structure and catalytic activity, *Inorganica Chimica Acta* (2017), doi: http://dx.doi.org/10.1016/j.ica.2017.06.064

Ruthenium^{II}(*p*-cymene) complexes bearing ligands of the type 1-[2'-(methoxycarbonyl)phenyl]-3-[4'-X-phenyl]triazenide (X= F, Cl, Br, I): synthesis, structure and catalytic activity

Erick Correa-Ayala[a], Carlos Campos-Alvarado[a], Daniel Chávez[a], David Morales-Morales[b], Simón Hernández-Ortega[b], Juventino J. García[c], Marcos Flores-Álamo[c], Valentín Miranda-Soto[a,*], Miguel Parra-Hake[a,*]

[a] *Centro de Graduados e Investigación, Instituto Tecnológico de Tijuana, Apartado Postal 1166, Tijuana, B.C. 22000, México*
[b] *Instituto de Química, Universidad Nacional Autónoma de México, Circuito Exterior.Cd. Universitaria Coyoacán, México D.F. 04510, México*
[c] *Facultad de Química, Universidad Nacional Autónoma de México, Circuito Exterior Cd. Universitaria Coyoacán, México D.F. 04510, México*

Abstract

The synthesis and characterization of triazenes of the type 1-[2'-(methoxycarbonyl)phenyl]-3-[4'-X-phenyl]triazene [X = F (**1**), Cl (**2**), Br (**3**), I (**4**)] as precursors of triazenide ligands for the preparation of their complexes of formula [Ru{1-(2'-methoxycarbonylphenyl)-3-(4'-X-phenyl)triazenide}(Cl)(*p*-cymene)] [X = F (**6**), Cl (**7**), Br (**8**), I (**9**), CH_3 (**10**)] are reported. Molecular structures for all four triazenes (**1-4**), and of complexes **6**, **9** and **10** were determined by X-ray diffraction studies. Complexes **6**-**10** were tested as catalysts in the transfer hydrogenation of acetophenone in the presence and in the absence of base. The best results were obtained in the presence of base with yields in the range of 86-94%, whereas even in the absence of base yields in the range 42-65% were achieved.

1. Introduction

There has been considerable attention on the coordination chemistry of 1,3-bis(aryl)triazenide ligands primarily because of their varied modes of binding [1,2]. These ligands can act as monodentate binding through a terminal [3,4] or central nitrogen [5,6], as bidentate to form a chelate [7,8], bidentate bridging two metal centers [9,10] or tricoordinate and tetracoordinate bridges [11,12] (Fig. 1).

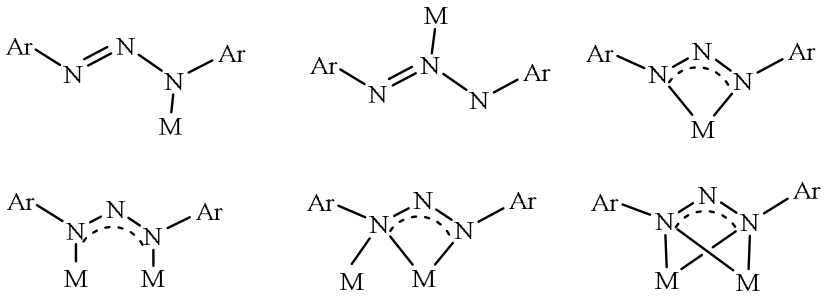

Figure 1. The coordination modes of the 1,3-bis(aryl)triazenide ligands.

Another reason for the current interest in 1,3-bis(aryl)triazenide ligands is their wide range of derivatives available through the addition of different substituents on the aryl group. In this direction, our research group has found that the incorporation of donor groups at the *ortho* position of the 1,3-bis(aryl)triazenide ligands can modify the coordination chemistry of the ligand [13-17] and the reactivity of their respective complexes [16,17], which in turn determine their catalytic activity.

Ru(*p*-cymene) complexes bearing 1,3-bis(aryl)triazenide ligands are attracting considerable interest from the point of view of their synthesis, structure, and catalytic and biological activity. Thus, Strähle and coworkers reported the synthesis and structure of the first complex of this type, [RuCl(η^2-1,3-ClC_6H_4NNNC_6H_4Cl)(η^6-*p*-cymene)] [18]. Albertin and coworkers, reported neutral complexes [RuCl(η^2-1,3-ArNNNAr)(η^6-*p*-cymene)], their structures and catalytic activity on hydrogenation of 2-cyclohexen-1-one and cynnamaldehyde under H_2 pressure [19]. Košmrlj, Osmak and coworkers have reported a series of 1,3-bis(aryl)triazenido(*p*-cymene)ruthenium(II) complexes with a high *in vitro* anticancer activity as the first study on the biological properties of this class of complexes [20].

As part of our ongoing research, we have recently reported a series of half-sandwich Ru(*p*-cymene) derivatives with symmetrically and unsymmetrically *ortho*-substituted 1,3-bis(aryl)triazenide ligands (Fig. 2), which proved to be catalytically active in the transfer hydrogenation of ketones in the absence or in the presence of base [21]. Furthermore, we found that the nature of the functional group at the *ortho* position of the 1,3-bis(aryl)triazenide ligands

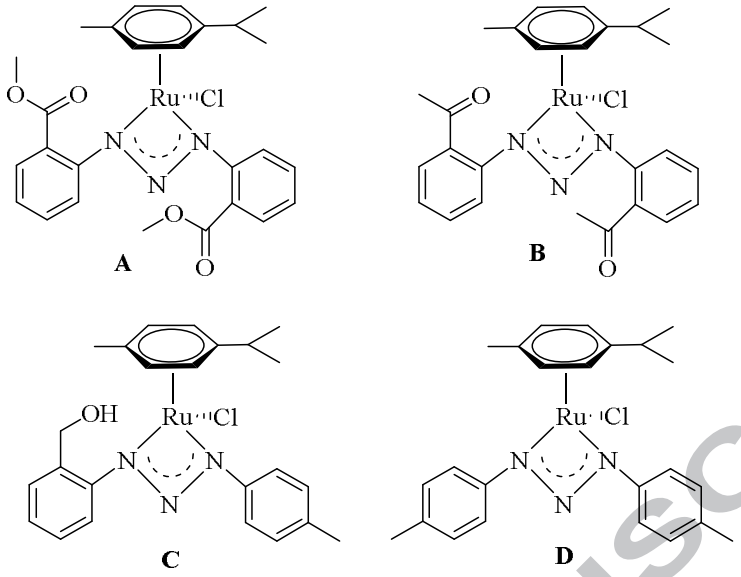

Figure 2. Ruthenium complexes previously reported [21].

can be tuned in order to modulate the catalytic properties of their complexes. The most promising result was the ability of complex **A** to catalyze the transfer hydrogenation of acetophenone under base-free conditions, since most pre-catalysts require a base to form the hydride complex as the active catalyst. Thus, reports in this area are rather scarce [22-25] and in most cases the precursors are hydride complexes [26-30] or an additive is required [31-33]. Based on those results, we turned our attention to analogues of complex **A** in which one of the *ortho*-methoxycarbonyl aryl groups was replaced by a halogen *para*-substituted aryl group with the aim of testing their catalytic activity. We hypothesized that these new complexes would be active catalysts in the transfer hydrogenation of ketones. It was expected that the relative catalytic efficiency to be dependent on the *para*-substituent.

Here we report on the synthesis of four new triazenes of the type 1-[2'-(methoxycarbonyl)phenyl]-3-[4'-X-phenyl]triazene (X = F, Cl, Br, I) as the triazenide ligand precursors, their ruthenium^{II}(*p*-cymene) complexes and results on the evaluation of these complexes as catalysts in the transfer hydrogenation of acetophenone, particularly under base free conditions.

2. Experimental Section

2.1. General comments

All synthetic work was carried out in air or under argon using standard Schlenk techniques or an inert atmosphere dry-box, where indicated. All solvents were dried over appropriate drying agents. $RuCl_3 \bullet 3H_2O$ (Aldrich) and other reagents are commercially available and were used as received. $[RuCl_2(p\text{-cymene})]_2$ [34] and {1-[2'-(methoxycarbonyl)phenyl]-3-[4'-(methyl)phenyl]}triazene (**5**) [15], were synthesized according to previously reported procedures. NMR spectra were recorded at 400 MHz with a Bruker Avance III spectrometer at 30 ºC unless otherwise specified. ^{1}H and ^{13}C NMR chemical shifts are reported in ppm referenced to residual solvent resonances (^{1}H NMR: 7.16 for C_6HD_5 in C_6D_6, 1.94 for CHD_2CN in CD_3CN, 2.05 for acetone-d_5 in acetone-d_6. ^{13}C NMR: 128.39, 1.39, and 29.92 for benzene-d_6, acetonitrile-d_3 and acetone-d_6, respectively). Coupling constants *J* are given in Hertz (Hz). IR spectra were recorded on a Perkin-Elmer FT-IR 1605 spectrophotometer. Melting points were measured in an Electrothermal GAC 88629 apparatus. Mass spectra were obtained by direct insertion on a Agilent Technologies 59756 Instrument. High Resolution Mass Spectrometry (HRMS) data were obtained in a micrOTOF-Q III MS instrument with electrospray ionization using sodium formate as calibrant.

2.2. Ligands

2.2.1. 1-[2'-(methoxycarbonyl)phenyl]-3-[4'-(fluoro)phenyl]triazene (**1**)

Methyl anthranilate (2.0 mL, 15.6 mmol) dissolved in water (5 mL) was mixed with 37% HCl (4.6 mL, 46.8 mmol) at 0 ºC, whereupon an aqueous solution (15%) of sodium nitrite (1.3 g, 18.7 mmol) was added dropwise with stirring. Once the amine was dissolved, a 15% solution of 4-(fluoro)aniline (1.7 g, 15.6 mmol) in methanol (11 mL) was added at 0 ºC, and the resulting solution stirred for 1 h. Then the reaction mixture was neutralized with a 15% aqueous solution of NaOAc (25 mL) to give a yellow precipitate. The product was purified by

crystallization at −5 ºC from a 9:1 ethyl acetate/hexane mixture to obtain a yellow crystalline solid (3.6 g, 13.4 mmol, 86%). MP = 109-112 ºC. IR(ATR): 3257, 3023, 2945, 1685, 1584, 1495, 1462, 1265, 1172, 1133, 1083, 837, 749 cm^{-1}. ^{1}H NMR [$CDCl_3$, 400 MHz]: δ 12.41 (s, 1H, NH), 8.01 (dd, *J* = 8.0, 1.6 Hz, 1H, Ar_{A3}), 7.90 (dd, *J* = 8.4, 0.8 Hz, 1H, Ar_{A6}), 7.59 (dd, *J* = 9.2, 5.2 Hz, 2H, $Ar_{B2,6}$), 7.50 (td, *J* = 7.6, 1.6 Hz, 1H, Ar_{A5}), 7.10 (t, *J* = 9.2 Hz, 2H, $Ar_{B3,5}$), 7.01 (td, *J* = 7.4, 1.2 Hz, 1H, Ar_{A4}), 3.94 (s, 3H, $OCH_{3(A8)}$). $^{13}C\{^{1}H\}$ NMR [$CDCl_3$, 100 MHz]: δ 168.6 (C_{A7}), 163.2 (d, J_{CF} = 244 Hz, C_{B4}), 147.1 (d, J_{CF} = 3 Hz, C_{B1}), 144.6 (C_{A1}), 135.6 (C_{A5}), 131.9 (C_{A3}), 124.2 (d, J_{CF} = 9 Hz, $C_{B2,6}$), 122.3 (C_{A4}), 116.7 (d, J_{CF} = 23 Hz, $C_{B3,5}$), 115.2 (C_{A6}), 112.8 (C_{A2}), 52.7 (C_{A8}). MS-EI *m/z* (%): 273 (9) $[M]^+$, 245 (33) $[M - N_2]^+$, 123 (73) $[M - NH(C_6H_4)COOCH_3]^+$, 95 (100) $[M - N_3H(C_6H_4)COOCH_3]^+$. HRMS (ESI-TOF) *m/z*: $[M+Na]^+$ Calcd for $C_{14}H_{12}FN_3O_2Na$ 296.0806; Found 296.0806.

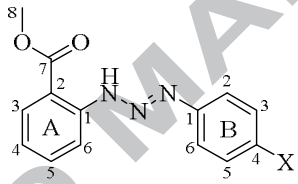

1, X = F; **2**, Cl; **3**, Br; **4**, I

2.2.2. 1-[2'-(methoxycarbonyl)phenyl]-3-[4'-(chloro)phenyl]triazene (**2**)

Ligand **2** was prepared in the same manner as triazene **1**, using 4-(chloro)aniline (2.0 g, 15.6 mmol) to obtain a yellow crystalline solid (3.3 g, 11.3 mmol, 72%). MP = 113-115 ºC. IR(ATR): 3243, 3023, 2938, 1685, 1583, 1500, 1455, 1263, 1158, 1086, 832, 752 cm^{-1}. ^{1}H NMR [$CDCl_3$, 400 MHz]: δ 12.41 (s, 1H, NH), 8.02 (dd, *J* = 8.0, 1.6 Hz, 1H, Ar_{A3}), 7.88 (dd, *J* = 8.4, 0.8 Hz, 1H, Ar_{A6}), 7.53 (d, *J* = 8.8 Hz, 2H, $Ar_{B2,6}$), 7.50 (td, *J* = 7.6, 1.6 Hz, 1H, Ar_{A5}), 7.35 (d, *J* = 8.8 Hz, 2H, $Ar_{B3,5}$), 7.03 (t, *J* = 7.6, 0.8 Hz, 1H, Ar_{A4}), 3.93 (s, 3H, $OCH_{3(A8)}$). $^{13}C\{^{1}H\}$ NMR [$CDCl_3$, 100 MHz]: δ 167.7 (C_{A7}), 148.3 (C_{B1}), 143.8 (C_{A1}), 134.6 (C_{A5}), 133.4 (C_{B4}), 131.3 (C_{A3}), 129.3 (C_{B3}), 123.0 (C_{B2}), 121.4 (C_{A4}), 114.7 (C_{A6}), 112.2 (C_{A2}), 52.3 (C_{A8}). EI-MS *m/z* (%): 291 (2) $[M + 2]^+$, 289 (13) $[M]^+$, 139 (81) $[M - NH(C_6H_4)COOCH_3]^+$, 111 (100) $[M - N_3H(C_6H_4)COOCH_3]^+$. HRMS (ESI-TOF) *m/z*: $[M + Na]^+$ Calcd for

$C_{14}H_{12}ClN_3O_2Na$ 312.0510; Found 312.0495. *Anal*. Calc. for $C_{14}H_{12}ClN_3O_2$ (289.06): C, 58.04; H, 4.18; N, 14.50%. Found: C, 57.76; H, 4.01; N, 14.63%.

2.2.3. 1-[2'-(methoxycarbonyl)phenyl]-3-[4'-(bromo)phenyl]triazene (**3**)

Ligand **3** was prepared in the same manner as triazene **1**, using 4-(bromo)aniline (2.7 g, 15.6 mmol) to obtain a yellow crystalline solid (9.2 g, 27.5 mmol, 71%). MP = 108-110 ºC. IR(ATR): 3255, 3071, 2945, 1685, 1581, 1500, 1455, 1261, 1153, 1004, 834, 753 cm^{-1}. ^1H NMR [$CDCl_3$, 400 MHz]: δ 12.42 (s, 1H, NH), 8.00 (dd, *J* = 8.0, 1.6 Hz, 1H, Ar_{A3}), 7.89 (dd, *J* = 8.4, 0.8 Hz, 1H, Ar_{A6}), 7.53 (t, 1H, Ar_{A5}), 7.52 (d, *J* = 8.8 Hz, 2H, $Ar_{B3,5}$), 7.48 (d, *J* = 8.8 Hz, 2H, $Ar_{B2,6}$), 7.03 (td, *J* = 7.6, 1.2 Hz, 1H, Ar_{A4}), 3.93 (s, 3H, $OCH_{3(A8)}$). $^{13}C\{^1H\}$ NMR [$CDCl_3$, 100 MHz]: δ 167.8 (C_{A7}), 148.5 (C_{B1}), 143.8 (C_{A1}), 134.6 (C_{A5}), 132.3 ($C_{B2,6}$), 131.3 (C_{A3}), 123.3 ($C_{B3,5}$), 121.54 (C_{A4}), 121.52 (C_{A4}), 114.7 (C_{A6}), 112.2 (C_{A2}), 52.3 (C_{A8}). EI-MS *m/z* (%): 335 (6) $[M + 2]^+$, 333 (6) $[M]^+$, 305 (1) $[M - N_2]^+$, 183 (62) $[M - NH(C_6H_4)COOCH_3]^+$, 155 (100) $[M - N_3H(C_6H_4)COOCH_3]^+$.

2.2.4. 1-[2'-(methoxycarbonyl)phenyl]-3-[4'-(iodo)phenyl]triazene (**4**)

Ligand **4** was prepared in the same manner as triazene **1**, using 4-(iodo)aniline (3.4 g, 15.6 mmol) to obtain a yellow crystalline solid (4.16 g, 10.92 mmol, 70%). MP = 126-128 ºC. IR(ATR): 3253, 3062, 2945, 1685, 1580, 1497, 1454, 1258, 1152, 1004, 832, 753 cm^{-1}. ^1H NMR [$CDCl_3$, 400 MHz]: δ 12.42 (s, 1H, NH), 8.02 (dd, *J* = 8.0, 1.6 Hz, 1H, Ar_{A3}), 7.89 (d, *J* = 8.4 Hz, 1H, Ar_{A6}), 7.72 (d, *J* = 8.4 Hz, 2H, $Ar_{B3,5}$), 7.52 (td, *J* = 8.0, 1.4 Hz, 1H, Ar_{A5}), 7.35 (d, *J* = 8.4 Hz, 2H, $Ar_{B2,6}$), 7.03 (t, *J* = 8.0 Hz, 1H, Ar_{A4}), 3.93 (s, 3H, $OCH_{3(A8)}$). $^{13}C\{^1H\}$ NMR [$CDCl_3$, 100 MHz]: δ 167.7 (C_{A7}), 149.4 (C_{B1}), 143.8 (C_{A1}), 138.3 ($C_{B2,6}$), 134.6 (C_{A5}), 131.3 (C_{A3}), 123.6 ($C_{B3,5}$), 121.5 (C_{A4}), 114.7 (C_{A6}), 112.3 (C_{A2}), 93.0 (C_{B4}), 52.1 (C_{A8}). EI-MS *m/z* (%): 381 (9) $[M]^+$, 353 (4) $[M - N_2]^+$, 231 (84) $[M - NH(C_6H_4)COOCH_3]^+$, 203 (100) $[M - N_3H(C_6H_4)COOCH_3]^+$. HRMS (ESI-TOF) *m/z*: $[M + Na]^+$ Calcd for $C_{14}H_{12}IN_3O_2Na$ 403.9866; Found 403.9865.

2.3. Synthesis of complexes

2.3.1. [Ru{1-(2'-methoxycarbonylphenyl)-3-(4'-fluorophenyl)triazenide}(Cl)(*p*-cymene)] (**6**)

1-[2'-(methoxycarbonyl)phenyl]-3-[4'-fluorophenyl]triazene (**1**) (44.6 mg, 0.1633 mmol, 2.0 eq) was dissolved in CH_2Cl_2 (5 mL) and triethylamine (33.0 mg, 0.3266 mmol, 4.0 eq) was added with stirring. Then, a solution of $[RuCl_2(p\text{-cymene})]_2$ (50.0 mg, 0.0816 mmol, 1.0 eq) in CH_2Cl_2 (5 mL) was slowly added and the mixture stirred for 24 h at room temperature. A dark yellow solution was formed, which was filtered through an alumina column. The solvent was removed under reduced pressure to obtain a yellow solid. Recrystallization by vapor diffusion of hexane into a concentrated solution of the product in THF at room temperature gave yellow crystals, suitable for X-ray diffraction analysis (64.0 mg, 0.1178 mmol, 72%). MP =108-110 ºC. IR(ATR): 3063, 2971, 1716, 1598, 1498, 1449, 1262, 1225, 1212, 1090, 837, 753 cm^{-1}. ^1H NMR [$(CD_3)_2CO$, 400 MHz]: δ 7.45 (td, *J* = 7.2, 1.6 Hz, 1H, Ar_{A5}), 7.39 (dd, *J* = 7.6, 1.2 Hz, 1H, Ar_{A3}), 7.27 (dd, *J* = 9.2, 4.8 Hz, 2H, $Ar_{B2,6}$), 7.24 (dd, *J* = 7.2, 0.8 Hz, 1H, Ar_{A6}), 7.14 (td, *J* = 7.6, 1.2 Hz, 1H, Ar_{A4}), 7.06 (t, *J* = 8.4 Hz, 2H, $Ar_{B3,5}$), 6.07 (d, *J* = 5.6 Hz, 1H, Ar_{C2}), 5.98 (d, *J* = 5.6 Hz, 1H, Ar_{C6}), 5.62 (d, *J* = 6.4 Hz, 2H, $Ar_{C3,5}$), 3.74 (s, 3H, $OCH_{3(A8)}$), 2.82 (sept, *J* = 6.8 Hz, 1H, CH_{C7}), 2.31 (s, 3H, $CH_{3(C10)}$), 1.29 (d, *J* = 6.8 Hz, 3H, $CH_{3(C8)}$), 1.28 (d, *J* = 6.8 Hz, 3H, $CH_{3(C9)}$). $^{13}C\{^1H\}$ NMR [$(CD_3)_2CO$, 100 MHz]: δ 170.1 (C_{A7}), 160.0 (d, J_{CF} = 240 Hz, C_{B4}), 146.0 (C_{A1}), 144.7 (d, J_{CF} = 2 Hz, C_{B1}), 131.8 (C_{A5}), 129.7 (C_{A3}), 124.4 (C_{A4}), 123.4 (C_{A6}), 123.3 (C_{A2}), 119.4 (d, J_{CF} = 8 Hz, $C_{B2,6}$), 116.2 (d, J_{CF} = 23 Hz, $C_{B3,5}$), 103.9 (C_{C1}), 102.7 (C_{C4}), 82.5 (C_{C6}), 82.0 (C_{C2}), 80.5 (C_{C3}), 80.2 (C_{C5}), 52.3 (C_{A8}), 32.5 (C_{C7}), 22.8 (C_{C8}), 22.7 (C_{C9}), 19.2 (C_{C10}). HRMS (ESI-TOF) *m/z*: $[M + Na]^+$ Calcd for $C_{24}H_{25}ClFN_3O_2RuNa$ 566.0558; Found 566.0564. *Anal*. Calc. for $C_{24}H_{25}ClFN_3O_2Ru$ (543.07): C, 53.09; H, 4.64; N, 7.73. Found: C, 52.92; H, 4.57; N, 7.29%.

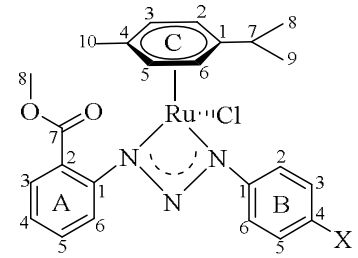

6, X = F; **7**, Cl; **8**, Br; **9**, I; **10**, CH_3

2.3.2. [Ru{1-(2'-methoxycarbonylphenyl)-3-(4'-chlorophenyl)triazenide}(Cl)(*p*-cymene)] (**7**)

Complex **7** was prepared in the same manner as complex **6**, using triazene **2** (47.2 mg, 0.1633 mmol, 2.0 eq). Yellow crystals (64.9 mg, 0.1160 mmol, 71%). MP = 145-147 ºC. IR(ATR): 3062, 2970, 1716, 1480, 1598, 1448, 1300, 1227, 1089, 833, 753 cm^{-1}. ^1H NMR [$CDCl_3$, 400 MHz]: δ 7.46 (td, *J* = 8.4, 1.6 Hz, 1H, Ar_{A5}), 7.40 (dd, *J* = 7.6, 1.2 Hz, 1H, Ar_{A3}), 7.29 (d, *J* = 8.4 Hz, 1H, Ar_{A6}), 7.27 (d, *J* = 8.8 Hz, 4H, $Ar_{B2,6,B3,5}$), 7.15 (td, *J* = 7.6, 1.2 Hz, 1H, Ar_{A4}), 6.06 (d, *J* = 6.4 Hz, 1H, Ar_{C2}), 5.98 (d, *J* = 6.4 Hz, 1H, Ar_{C6}), 5.63-5.60 (m, 2H, $Ar_{C3,5}$), 3.74 (s, 3H, $OCH_{3(A8)}$), 2.82 (sept, *J* = 6.8 Hz, 1H, CH_{C7}), 2.30 (s, 3H, $CH_{3(C10)}$), 1.28 (d, *J* = 6.8 Hz, 3H, $CH_{3(C8)}$), 1.27 (d, *J* = 6.8 Hz, 3H, $CH_{3(C9)}$). $^{13}C\{^1H\}$ NMR [$(CD_3)_2CO$, 100 MHz]: δ 170.0 (C_{A7}), 146.9 (C_{B1}), 145.8 (C_{A1}), 131.8 (C_{A5}), 129.7 (C_{A3}), 129.5 ($C_{B3,5}$), 129.4 (C_{A2}), 124.8 (C_{A4}), 123.5 (C_{A6}), 123.4 (C_{B4}), 119.3 ($C_{B2,6}$), 103.9 (C_{C1}), 102.8 (C_{C4}), 82.5 (C_{C6}), 82.0 (C_{C2}), 80.5 (C_{C3}), 80.2 (C_{C5}), 52.3 (C_{A8}), 32.5 (C_{C7}), 22.8 (C_{C8}), 22.7 (C_{C9}), 19.2 (C_{C10}). HRMS (ESI-TOF) *m/z*: $[M + Na]^+$ Calcd for $C_{24}H_{25}Cl_2N_3O_2RuNa$ 582.0260; Found 582.0265. *Anal*. Calc. for $C_{24}H_{25}Cl_2N_3O_2Ru$ (559.04) + C_3H_6O (acetone) : C, 52.51; H, 5.06; N, 6.80. Found: C, 52.76; H, 5.02; N, 6.50%.

2.3.3. [Ru{1-(2'-methoxycarbonylphenyl)-3-(4'-bromophenyl)triazenide}(Cl)(*p*-cymene)] (**8**)

Complex **8** was prepared in the same manner as complex **6**, using triazene **3** (54.4 mg, 0.1633 mmol, 2.0 eq). Yelow crystals (69.1 mg, 0.1144 mmol, 70%). MP = 150-155 ºC. IR(ATR): 3061, 2971, 1717, 1598, 1478, 1449, 1300, 1227, 1067, 831, 753 cm^{-1}. ^1H NMR [$(CD_3)_2CO$, 400 MHz]: δ 7.47 (td, *J* = 7.2, 1.6 Hz, 1H, Ar_{A5}), 7.44 (d, *J* = 8.8 Hz, 2H, $Ar_{B3,5}$), 7.41 (dd, *J* = 7.6, 1.2 Hz, 1H, Ar_{A3}), 7.28 (dd, *J* = 8.0, 0.8 Hz, 1H, Ar_{A6}), 7.21 (d, *J* = 8.8 Hz,

2H, $Ar_{B2,6}$), 7.17 (td, *J* = 7.6, 1.2 Hz, 1H, Ar_{A4}), 6.08 (d, *J* = 5.6 Hz, 1H, Ar_{C2}), 5.98 (d, *J* = 5.6 Hz, 1H, Ar_{C6}), 5.62-5.60 (m, 2H, $Ar_{C3,5}$), 3.75 (s, 3H, $OCH_{3(A8)}$), 2.82 (sept, *J* = 6.8 Hz, 1H, CH_{C7}), 2.31 (s, 3H, $CH_{3(C10)}$) 1.29 (d, *J* = 6.8 Hz, 3H, $CH_{3(C8)}$), 1.28 (d, *J* = 6.8 Hz, 3H, $CH_{3(C9)}$). $^{13}C\{^1H\}$ NMR [$(CD_3)_2CO$, 100 MHz]: δ 170.2 (C_{A7}), 147.4 (C_{B1}), 145.8 (C_{A1}), 132.5 ($C_{B3,5}$), 131.8 (C_{A5}), 129.8 (C_{A3}), 124.8 (C_{A4}), 123.6 (C_{A6}), 123.4 (C_{A2}), 119.7 ($C_{B2,6}$), 117.1 (C_{B4}), 104.0 (C_{C1}), 102.8 (C_{C4}), 82.5 (C_{C6}), 82.1 (C_{C2}), 80.6 (C_{C3}), 80.3 (C_{C5}), 52.3 (C_{A8}), 32.5 (C_{C7}), 22.8 (C_{C8}), 22.7 (C_{C9}), 19.4 (C_{C10}). HRMS (ESI-TOF) *m/z*: $[M + Na]^+$ Calcd for $C_{24}H_{25}ClBrN_3O_2RuNa$ 627.9745; Found 627.9749. $[M - Cl]^+$ Calcd for $C_{24}H_{25}BrN_3O_2Ru$ 570.0164; Found 570.0165.

2.3.4. [Ru{1-(2'-methoxycarbonylphenyl)-3-(4'-iodophenyl)triazenide}(Cl)(*p*-cymene)] (**9**)

Complex **9** was prepared in the same manner as complex **6**, using triazene **4** (62.2 g, 0.1633 mmol, 2.0 eq). Yellow crystals (78.0 mg, 0.1198 mmol, 74%). MP = 158-160 ºC. IR(ATR): 3062, 2947, 1712, 1594, 1574, 1474, 1444, 1300, 1299, 1124, 1067, 834, 753 cm^{-1}. ^1H NMR [$(CD_3)_2CO$, 400 MHz]: δ 7.63 (d, *J* = 8.8 Hz, 2H, $Ar_{B3,5}$), 7.47 (td, *J* = 7.6, 1.6 Hz, 1H, Ar_{A5}), 7.41 (dd, *J* = 7.6, 1.2 Hz, 1H, Ar_{A3}), 7.28 (dd, *J* = 8.0, 1.2 Hz, 1H, Ar_{A6}), 7.18 (td, *J* = 7.6, 1.2 Hz, 1H, Ar_{A4}), 7.08 (d, *J* = 8.8 Hz, 2H, $Ar_{B2,6}$), 6.10 (d, *J* = 6.0 Hz, 1H, Ar_{C2}), 6.00 (d, *J* = 6.0 Hz, 1H, Ar_{C6}), 5.63-5.60 (m, 2H, $Ar_{C3,5}$), 3.75 (s, 3H, $OCH_{3(A8)}$), 2.82 (sept, *J* = 6.8 Hz, 1H, $CH_{3(C7)}$), 2.32 (s, 3H, $CH_{3(C10)}$), 1.29 (d, *J* = 6.8 Hz, 3H, $CH_{3(C8)}$), 1.28 (d, *J* = 6.8 Hz, 3H, $CH_{3(C9)}$). $^{13}C\{^1H\}$ NMR [$(CD_3)_2CO$, 100 MHz]: δ 170.0 (C_{A7}), 148.0 (C_{B1}), 146.0 (C_{A1}), 138.7 ($C_{B3,5}$), 131.9 (C_{A5}), 129.9 (C_{A3}), 125.0 (C_{A4}), 123.7 (C_{A6}), 123.5 (C_{A2}), 120.2 ($C_{B2,6}$), 104.2 (C_{C1}), 103.0 (C_{C4}), 87.7 (C_{B4}), 82.6 (C_{C6}), 82.2 (C_{C2}), 80.7 (C_{C3}), 80.4 (C_{C5}), 52.4 (C_{A8}), 32.6 (C_{C7}), 22.9 (C_{C8}), 22.8 (C_{C9}), 19.3 (C_{C10}). HRMS (ESI-TOF) *m/z*: $[M + Na]^+$ Calcd for $C_{24}H_{25}ClIN_3O_2RuNa$ 673.9619; Found 673.9621. $[M - Cl]^+$ Calcd for $C_{24}H_{25}IN_3O_2Ru$ 616.0036; Found 616.0040. *Anal*. Calc. for $C_{24}H_{25}ClIN_3O_2Ru$ (650.97): C, 44.29; H, 3.87; N, 6.46. Found: C, 44.31; H, 3.84; N, 6.16%.

2.3.6. [Ru{1-(2'-methoxycarbonylphenyl)-3-(4'-methylphenyl)triazenide}(Cl)(*p*-cymene)] (**10**)

Complex **10** was prepared in the same manner as complex **6**, using triazene **5** (43.9 mg, 0.1633 mmol, 2.0 eq). Yellow crystals (81.0 mg, 0.1502 mmol, 93%). MP = 129-132 ºC. IR(ATR): 3064, 2970, 2939, 1720, 1593, 1447, 1297, 1094, 759 cm^{-1}. ^{1}H NMR [$(CD_3)_2CO$, 400 MHz]: δ 7.43 (td, *J* = 8.4, 1.6 Hz, 1H, Ar_{A5}), 7.35 (dd, *J* = 7.6, 1.2 Hz, 1H, Ar_{A3}), 7.23 (dd, *J* = 8.4, 0.8 Hz, 1H, Ar_{A6}), 7.18 (d, *J* = 8.4 Hz, 2H, $Ar_{B2,6}$), 7.14 (td, *J* = 7.6, 1.2 Hz, 1H, Ar_{A4}), 7.10 (d, *J* = 8.4 Hz, 2H, $Ar_{B3,5}$), 6.04 (d, *J* = 5.6 Hz, 1H, Ar_{C6}), 5.96 (d, *J* = 5.6 Hz, 1H, Ar_{C2}), 5.59 (d, *J* = 6.4 Hz, 1H, $Ar_{C3,5}$), 3.74 (s, 3H, $OCH_{3(A8)}$), 2.79 (sept, *J* = 6.8 Hz, 1H, CH_{C7}), 2.30 (s, 3H, $CH_{3(C10)}$), 2.29 (s, 3H, $CH_{3(B7)}$), 1.29 (d, *J* = 6.8 Hz, 6H, $CH_{3(C8)}$), 1.28 (d, *J* = 6.8 Hz, 6H, $CH_{3(C9)}$). $^{13}C\{^{1}H\}$ NMR [$(CD_3)_2CO$, 100 MHz]: δ 170.3 (C_{A7}), 146.2 (C_{A1}), 145.9 (C_{B1}), 134.7 (C_{B4}), 131.7 (C_{A5}), 130.1 ($C_{B3,5}$), 129.7 (C_{A3}), 124.0 (C_{A4}), 123.2 (C_{A2}), 123.1 (C_{A6}), 118.0 ($C_{B2,6}$), 103.7 (C_{C1}), 102.7 (C_{C4}), 82.5 (C_{C2}), 82.1 (C_{C6}), 80.5 (C_{C5}), 80.2 (C_{C3}), 52.2 (C_{A8}), 32.5 (C_{C7}), 22.8 (C_{C8}), 22.7 (C_{C9}), 20.9 (C_{B7}), 19.2 (C_{C10}). HRMS (ESI-TOF) *m/z*: $[M + Na]^+$ Calcd for $C_{25}H_{28}ClN_3O_2RuNa$ 562.0809; Found 562.0804.

2.4. X-ray crystallography

A suitable single crystal of **1**, **3**, **4**, **6**, **9** and **10** was mounted on a glass fiber and data were collected with an Oxford Diffraction Gemini "A" diffractometer with a CCD area detector, with radiation source of $\lambda_{MoK\alpha}$ = 0.71073 Å for **3**, **4**, **6**, **9** and **10** and $\lambda_{CuK\alpha}$ = 1.54184 Å and using graphite-monochromatized radiation at 298 K for **9** and **10**, and 130 K for **1**, **3**, **4** and **6**. Unit cell parameters were determined with a set of three runs of 15 frames (1° in ω). The double pass method of scanning was used to exclude any noise. The collected frames were integrated by using an orientation matrix determined from the narrow frame scans. CrysAlisPro and CrysAlis RED software packages were used for data collection and integration [35]. The double pass method of scanning was used to exclude any noise. The collected frames were integrated by using an orientation matrix determined from the narrow frame scans. Final cell constants were determined by a

global refinement; collected data were corrected for absorbance by using analytical numeric absorption correction using a multifaceted crystal model based on expressions upon the Laue symmetry using equivalent reflections [36]. Structure solution and refinement were carried out with the SHELXS-2014 and SHELXL-2014 packages [37]; WinGX v2014.1 software was used to prepare material for publication [38,39]. Full-matrix least-squares refinement was carried out by minimizing $(Fo^2 - Fc^2)^2$. All nonhydrogen atoms were refined anisotropically and the refinement was carried out without restraint. The H atom of the amine group was located in a difference map and refined isotropically with U*iso*(H) = 1.2 for H–N. Hydrogen atoms attached to carbon atoms were placed in geometrically idealized positions and refined as riding on their parent atoms, with C—H = 0.93–0.98 Å with U*iso* (H) = 1.2 Ueq(C) for methyne and aromatic groups, and U*iso* (H) = 1.5 U*eq*(C) for methyl group.

A suitable crystal of compound **2** was mounted on a glass fiber at room temperature, then placed on a Bruker SMART APEX CCD-based X-ray diffractometer system equipped with a Mo-target X-ray tube ($\lambda_{MoK\alpha}$ = 0.71073 Å). The detector was placed at a distance of 5.0 cm from the crystals, in all cases decay was negligible. A total of 2400 frames were collected with a scan width of 0.3 in *x* and an exposure time of 10 s/frame. The frames were integrated with the Bruker SAINT Software package using a narrow-frame integration algorithm. Systematic absences and intensity statistics were used in space group determination. The structure was solved using direct methods using SHELXS-2014/7 program [40]. Anisotropic structure refinements were achieved using full matrix, least-squares technique on all non-hydrogen atoms. All hydrogen atoms were placed in idealized positions, based on hybridization, with isotropic thermal parameters fixed at 1.2 times the value of the attached atom. Structure refinements were performed using SHELXL-2014/7 [40].

The crystal structure is almost planar, azido frame is making dihedral angles of 4.5 (2)° and 4.9 (2)° with the aromatic ring (C1-C6) and (C9-C14), the dihedral angle between phenyl ring was 7.3 (2)°.

2.5. General procedure for transfer hydrogenation studies monitored by ^{1}H NMR

All measurements were made on a Bruker 400 spectrometer operating at 400 MHz. Inside a nitrogen glovebox acetophenone (6×10^{-5} mol), 1,3,5-trimethylbenzene (2 μL) as internal standard and 0.6 mL of 2-propanol-d_8 were transferred into a J-Young NMR tube. The tube was closed in order to avoid air contamination, and a ^{1}H NMR spectrum was recorded. Next, the tube was brought back into the glovebox and the ruthenium precatalyst (1.2×10^{-6} mol) and KOH (6×10^{-6} mol only for base-assisted reactions) were added. Outside of the glovebox the tube was placed in an oil bath at 70 °C. At the desired sampling time, the tube was taken out of the oil bath, and a ^{1}H NMR spectrum was recorded. Percent conversions were determined by comparing the integration of the aromatic protons at the *ortho* position of the alcohol with the aromatic protons at the *ortho* position of the acetophenone. The value of the integral for the singlet due to the aromatic protons of 1,3,5-trimethylbenzene (internal standard) was set equal to 10 units in each case.

2.6 General procedure for catalytic transfer hydrogenation monitored by Gas Chromatography-Mass Spectrometry (GC-MS).

Ruthenium precatalyst (1.2×10^{-6} mol), acetophenone (6×10^{-5} mol), 2-propanol (0.6 mL) and KOH (6×10^{-6} mol only for base-assisted reactions) were transferred into a 1.5 mL vial. The resulting solution was heated at 70 ºC and the reaction progress was monitored by GC-MS analysis in order to calculate the conversion of the substrate. At the desired sampling time, an aliquot of 0.1 mL was taken and diluted to 1.0 mL with 2-propanol.

The analytical GC-MS system used was an Agilent 7890A GC coupled to 5975C Mass detector Agilent Technologies, equipped with a HP-5MS capillary column (30 m × 0.25 mm × 0.25 micron) Agilent Technologies, Inc. An Agilent Technologies 7693 auto sampler was used to inject 1 μL of a solution sample. The ionization energy was 70 eV with a mass range of 30 to

800 m/z. The initial temperature of the column was set at 80 ºC, held for 2 min, and then a ramp of 15 ºC/min to 250 ºC. The temperature of the injector was set at 250 ºC and the detector to 230 ºC. The flow rate of the carrier gas (Helium) was 1.0 mL/min injected with a gas dilution of 1:50. Identification of the individual components was based on comparison with the mass spectra library (NIST98).

3. Results and discussion

3.1. Synthesis and general characterization

3.1.1. Triazenes

Triazene **5** was synthesized according to previously reported procedure [15], while triazenes **1**-**4** were synthesized following modified literature procedures [41] by diazotization of methyl antranilate with sodium nitrite, followed by coupling with the corresponding *p*-substituted aniline. The structures with atom labeling of triazenes **1**-**4** are shown in Fig. 3.

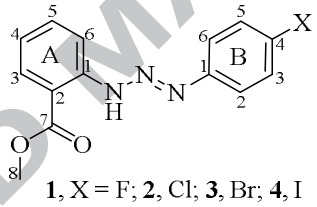

1, X = F; **2**, Cl; **3**, Br; **4**, I

Figure 3. Structure and labeling of triazenes **1-4**.

The IR spectra of triazenes **1**-**4** show bands in common in the range of 3243-3188 cm^{-1} for the N-H group, 1582-1576 cm^{-1} for the N_3 system and at 1685 cm^{-1} for the C=O group.

The ^1H NMR spectra of triazenes **1-4** show a broad singlet at low field in the range of 12.33-12.42 ppm assigned to the triazene N-H group. In the aromatic region of each triazene, there are two doublets and two triplets at ~8.01, ~7.89, ~7.52 and ~7.03 ppm, respectively, which correspond to the *ortho*-disubstituted aromatic ring (A). On the other hand, the two doublets of the *para*-disubstituted aromatic ring (B) appear at different chemical shifts as a result of differences in the electronegativity of the *para*-substituent. For example, the signal of the equivalent hydrogen atoms B3 and B5 appears at 7.10, 7.35, 7.52 and 7.72 ppm for triazenes **1** (*p*-F), **2** (*p*-Cl), **3** (*p*-Br), and **4** (*p*-I), respectively (Fig. 4). These results are in agreement with

the experimental and calculated chemical shifts of a related triazene [42]. The signal of the methoxy group (OCH_3) appears as a singlet at ~3.93 ppm, which integrates for three hydrogens. The ^{13}C NMR spectra of triazenes **2**-**4** show 10 signals for the carbon atoms in the aromatic region, a carbonyl signal at 167.7 ppm, and a methoxy signal at ~52.2 ppm for the *ortho*-methoxycarbonyl group. On the other hand, in the ^{13}C NMR spectrum of triazene **1**, the carbons B4 (163.2 ppm), B3,5 (116.7 ppm), B2,6 (124.2 ppm) and B1 (147.1 ppm), appear as doublets with coupling constants of 244.3, 22.7, 9.0 and 3.0 Hz, respectively, due to their coupling with the *p*-F substituent. Interestingly, the inductive effect of the halogen substituent affects the chemical shift of carbon B4 [43], which is shifted downfield as the halogen bonded to carbon B4 becomes more electronegative, appearing at 163.2, 133.4, 121.5 and 93.0 ppm for triazenes **1** (*p*-F), **2** (*p*-Cl), **3** (*p*-Br), and **4** (*p*-I), respectively.

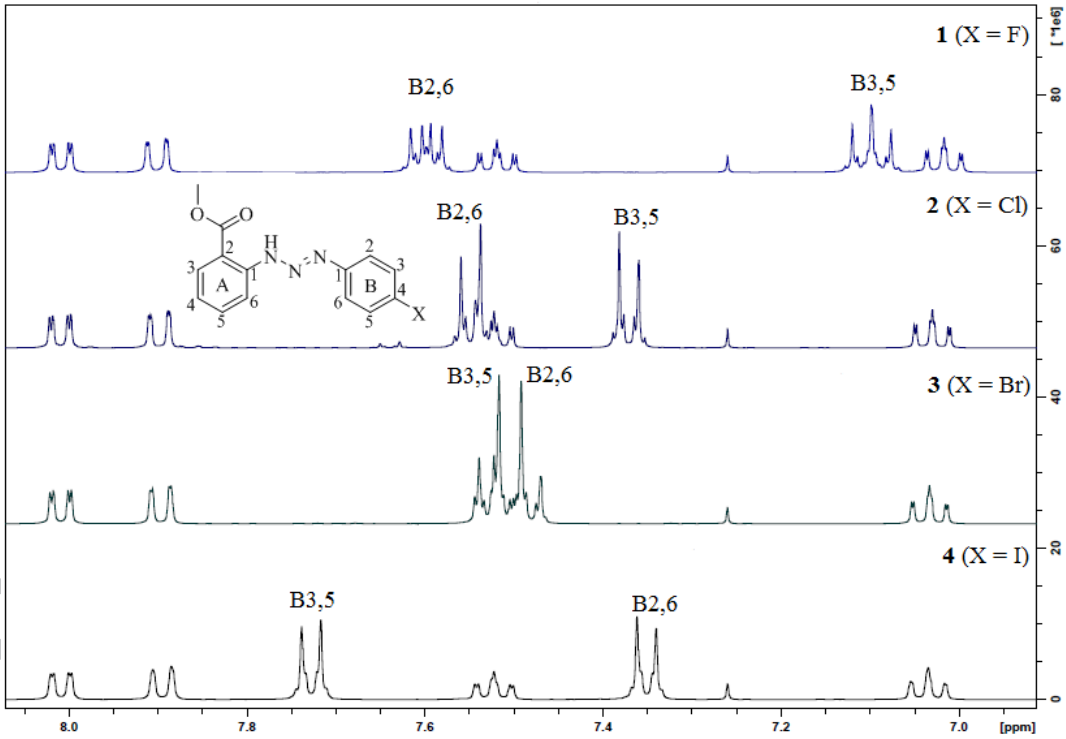

Figure 4. ^{1}H NMR spectra of the aromatic region of triazenes **1-4**.

3.1.2. Ruthenium Complexes

Reaction of 1,3-bis(aryl)triazene ligand precursors **1-5** with half equivalent of [RuCl(*p*-cymene)(μ-Cl)]$_2$ in dichloromethane at room temperature and in the presence of triethylamine, resulted in the formation of new monomeric [RuCl(η^2-1,3-ArNNNAr)(η^6-*p*-cymene)] complexes **6-10** (Eq. (1)).

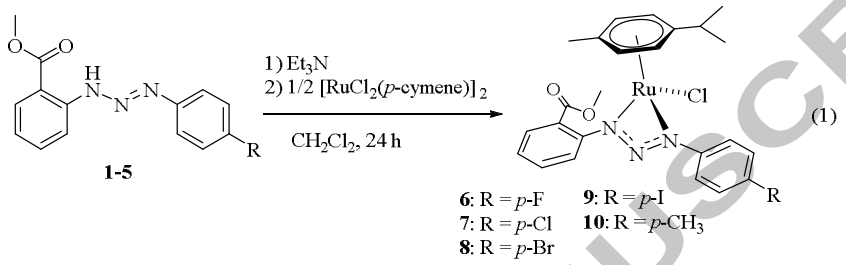

Complexes **6-10** were isolated as stable yellow solids. Their formulation is supported by analytical and spectroscopic data (IR, NMR and HRMS), and X-ray crystal structure determination.

The IR spectra show bands in the range of 1598-1593 and 1720-1716 cm^{-1} for the triazenide (N_3) system and carbonyl group, respectively. The ν(C=O) bands undergo positive shifts with respect to the triazenes **1-5**, suggesting that the carbonyl group remains uncoordinated [44-46].

In the ^{1}H NMR spectra of **6-10**, the triazenide ligands give signals for *ortho* and *para*-disubstituted aromatic rings shifted 0.1-0.6 ppm downfield, in comparison with their respective free triazenes **1-5**. The methoxy group is observed as a singlet at ~3.75 ppm. In the ^{13}C NMR spectra of complexes **6-10**, no significant shifts were observed compared to the free triazenes **1-5**.

Interestingly, the presence of a chiral center in the metal complexes **6-10** due to the coordination of the unsymmetric triazenide ligands from **1-5**, is clearly reflected in their ^{1}H NMR spectra. The *p*-cymene aromatic protons are observed as two doublets in the range of 6.10-5.70 ppm (J = ~6.0 Hz) and two overlapped doublets at ~5.62 ppm, which is typical in Ru^{II}(*p*-cymene) complexes where the metal is a chiral center [47-51]. With symmetric triazenide

ligands in Ru^{II}(*p*-cymene)triazenide complexes previously reported [19-21], these aromatic protons are two by two equivalent, leading to only two signals in the spectra. Also, the isopropyl methyl protons are inequivalent, appearing as two doublets (J = ~6.8 Hz) at ~1.29 and ~1.28 ppm. In the ^{13}C NMR spectra, the signals for the isopropyl methyl carbons are observed as two signals at ~22.8 and ~22.7 ppm, while the *p*-cymene aromatic carbons are observed as six signals in the range of 104.0-80.2 ppm. The NMR assignments were confirmed by gCOSY, gHSQC and gHMBC experiments (see Supporting Information). Complexes **6-10** were analyzed by HRMS (ESI-TOF) and their spectra showed the formation of adducts of the type $[M + Na]^+$, which may be a consequence of using sodium formate as calibrant.

3.2. Description of the crystal structures

Crystals of triazenes **1-4** suitable for X-ray diffraction studies were obtained. Triazenes **3** and **4** crystallized in the triclinic crystalline system while **1** and **2** in the monoclinic and orthorhombic system, respectively, with different space groups (P 21/n for **1**, P 21 21 21 for **2**, and P-1 for **3** and **4**).

Since the structures of triazenes **1**-**4** are analogous, only the ORTEP diagram of triazene **1** in Fig. 5 is shown as an example. The ORTEP diagrams of triazenes **2**-**4** and the crystal data for these compounds are given in the Supporting information (Figures S1-3 and Table S1, respectively), while selected bond distances and angles are listed in Table 1. Triazenes **1**-**4** adopt *trans* configuration about the N=N double bond. The N(1)-N(2) and N(2)=N(3) bond lengths are ca. 1.34 and 1.26 Å, respectively, which indicates the presence of single and double bonds. The N(1)-N(2)=N(3) bond angles are ca. 111.0°, whereas the dihedral angle between the two aromatic rings at 5.68, 7.27, 13.04 and 14.89°, for triazenes **1-4**, respectively, seems to be affected by the electronegativity of the *para*-substituent. The bond distances and angles are in agreement with those reported for related triazenes with *ortho* and *para*-halogen substituents [52-58]. On the other hand the distances and angles of the *o*-methoxycarbonyl substituent are in agreement with those reported for related triazenes [59,60].

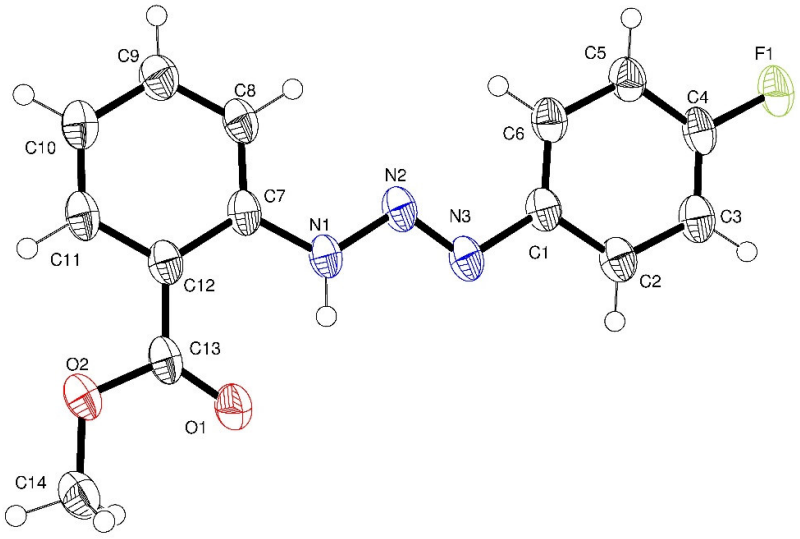

Figure 5. ORTEP diagram for triazene **1** with thermal ellipsoids drawn at 50% probability level.

Table 1. Selected bond distances (Å) and angles (°) for triazenes **1-4**.

Bond distances (Å)				
	1 (X = F)	**2** (X = Cl)	**3** (X = Br)	**4** (X = I)
N(1)-N(2)	1.347(4)	1.340(2)	1.345(3)	1.334(5)
N(2)-N(3)	1.270(5)	1.261(2)	1.264(3)	1.262(4)
N(1)-H(1D)	0.907(19)	0.915(9)	0.896(17)	0.81(4)
C(7)-N(1)	1.397(5)	1.378(3)	1.384(3)	1.389(5)
C(1)-N(3)	1.425(5)	1.418(3)	1.424(3)	1.414(5)
C(4)-X	1.368(4)	1.740(2)	1.903(3)	2.108(4)
C(13)=O(1)	1.232(5)	1.202(3)	1.215(3)	1.213(4)
C(13)-O(2)	1.341(4)	1.330(3)	1.337(3)	1.345(5)
C(14)-O(2)	1.446(5)	1.434(2)	1.449(3)	1.445(5)
		Angles (°)		
N(3)-N(2)-N(1)	111.1(3)	112.1(2)	111.0(2)	112.3(3)
N(2)-N(3)-C(1)	111.6(3)	113.1(2)	112.5(2)	112.1(3)
N(2)-N(1)-C(7)	119.4(3)	121.3(2)	120.2(2)	120.6(4)
N(2)-N(1)-H(1D)	122(3)	120.7(15)	119.4(18)	121(3)
O(1)-C(13)-O(2)	121.6(4)	123.3(3)	121.6(3)	121.8(4)

Crystals of the triazenide ruthenium complexes **6**, **9** and **10** suitable for X-ray diffraction were obtained by vapor phase diffusion of hexane into concentrated solutions of the complexes in tetrahydrofuran. Complexes **6** and **9** crystallized in the monoclinic crystalline system while **10** in the orthorhombic system, with different space groups (P 21/n, P 21/c and P 21 21 21, respectively).

The ORTEP diagrams of complexes **6**, **9** and **10** are given in Figs. 6-8 with selected bond lengths and angles. The crystal data for these compounds are given in the Supporting information, (Table S2). In the complexes the ruthenium atom is surrounded by the η^6-bonded *p*-cymene ring, a chelating η^2-triazenide ligand and one chloro ligand, attaining a pseudo-octahedral ¨three legged piano stool¨ geometry. The small-bite of the triazenide [N(1)-Ru-N(2)] of ca. 59.0°, influence the bond angles around the metal, but only those affecting this ligand, in such a way that the N-Ru-Cl angles are all close to the expected 90°. The Ru-N distances are ca 2.06 Å, while the N-N bond lengths in the triazenide systems are ~1.31 Å, a value which is between a single (N-N) and a double bond (N=N). All these values are in the range found for previously reported Ru^{II}(*p*-cymene)triazenide complexes [18-21].

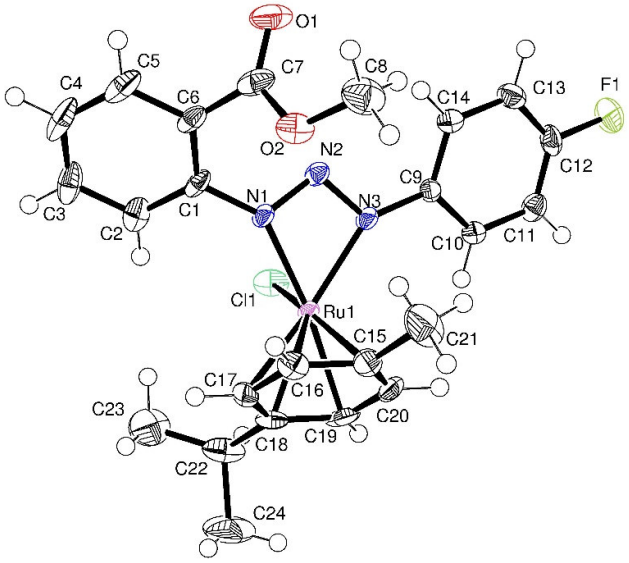

Figure 6. ORTEP diagram for compound **6** with thermal ellipsoids drawn at 60% probability level. Bond distances (Å): Ru-N1, 2.067(2); Ru-N3, 2.084(2); N(1)-N(2), 1.306(3); N(2)-N(3), 1.314(3); N(1)-C(1), 1.398(3); Ru-Cl1, 2.3897(7); Ru-CT, 1.668; C(7)=O(1), 1.211(5); C(12)-F(1), 1.370(3). Bond angles (°): N(1)-N(2)-N(3), 103.0(2); N1-Ru-N3, 59.19(8); Cl-Ru-N1, 85.51(6); Cl-Ru-N3, 87.83(7); O(2)-C(13)=O(1), 122.8(3).

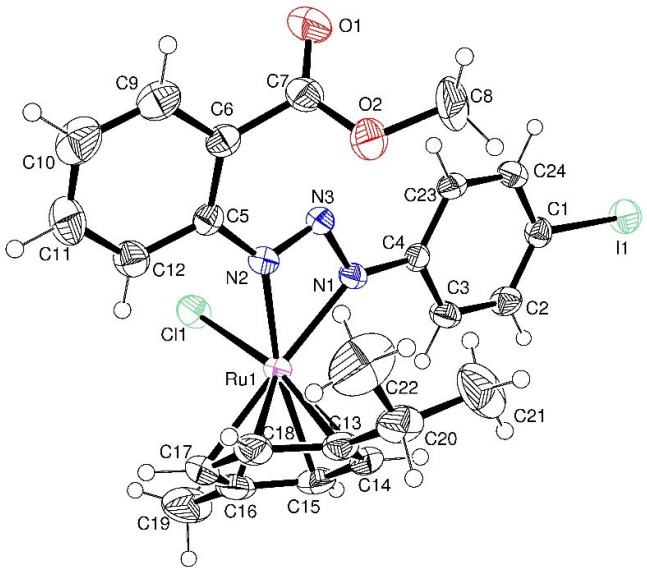

Figure 7. ORTEP diagram for the compound **9** with thermal ellipsoids drawn at 40% probability level. Bond distances (Å): Ru-N1, 2.076(2); Ru-N3, 2.074(2); N(1)-N(2), 1.303(3); N(2)-N(3), 1.316(3); N(1)-C(1), 1.409(3); Ru-Cl1, 2.3895(8); Ru-CT, 1.675; C(7)=O(1), 1.199(4); C(12)-I(1), 2.102(3). Bond angles (°): N(1)-N(2)-N(3), 102.3(2); N1-Ru-N3, 58.84(10); Cl-Ru-N1, 87.46(7); Cl-Ru-N3, 83.77(7); O(2)-C(7)=O(1), 125.1(3).

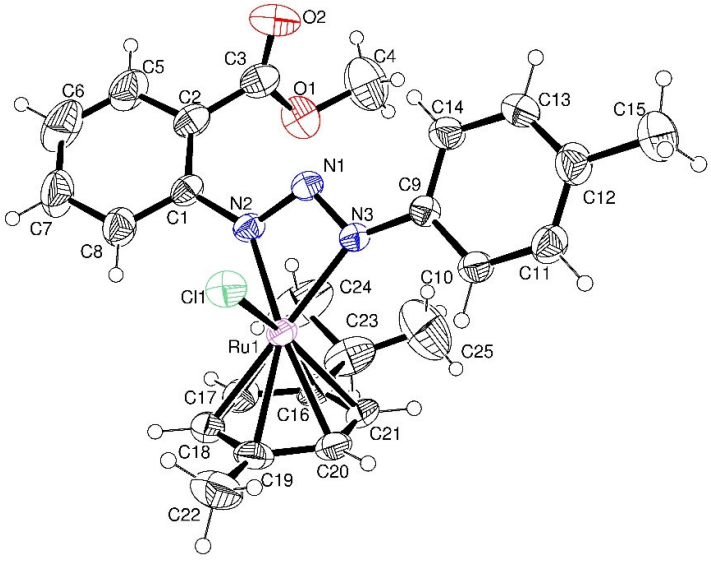

Figure 8. ORTEP diagram for compound **10** with thermal ellipsoids drawn at 40% probability level. Bond distances (Å): Ru-N1, 2.066(4); Ru-N3, 2.089(4); N(1)-N(2), 1.312(5); N(2)-N(3), 1.322(6); N(1)-C(1), 1.400(6); Ru-Cl(1), 2.3921(13); Ru-CT, 1.671; C(7)=O(1), 1.193(8). Bond angles (°): N(1)-N(2)-N(3), 102.0(4); N1-Ru-N3, 59.03(16); Cl-Ru-N1, 84.76(12); Cl-Ru-N3, 85.44(11); O(2)-C(7)=O(1), 123.4(7).

These complexes display interesting crystal arrangements. For example, complex **6** exhibits C-H···Cl, C-H···F and C-H···π important intermolecular hydrogen bonding interactions that define the crystal arrangement. The C9-H9···Cl [2.907 Å, 158.6°] interaction gives place to the formation of a centrosymmetric 14-member ring shown in Fig. 9. In addition, the Cl atom presents a second C-H···Cl interaction with H3 [2.86, 137°], which together with the C4-H4···π_{C7-C12} [2.99 Å, 130°] interactions produces a 10-member cycle (Fig. 9). Thus, both the 14-member and the 10-member rings form a 2D-supramolecular arrangement shown in Fig. 10. The supramolecular framework is completed by C24-H24A···F [2.76 Å, 117.5°] and C19-H19···π_{C1-C6} [2.88 Å, 111°] interactions.

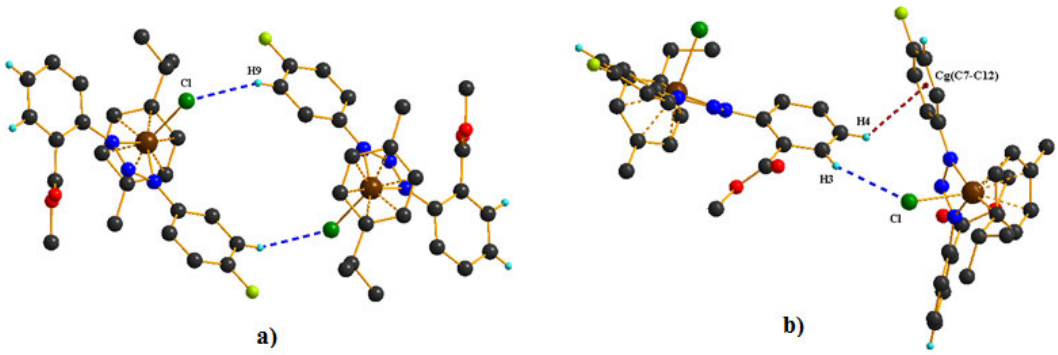

Figure 9. Representation of the 14-member (a) and 10-member (b) rings in complex **6**. Hydrogen atoms not involved have been omitted for clarity.

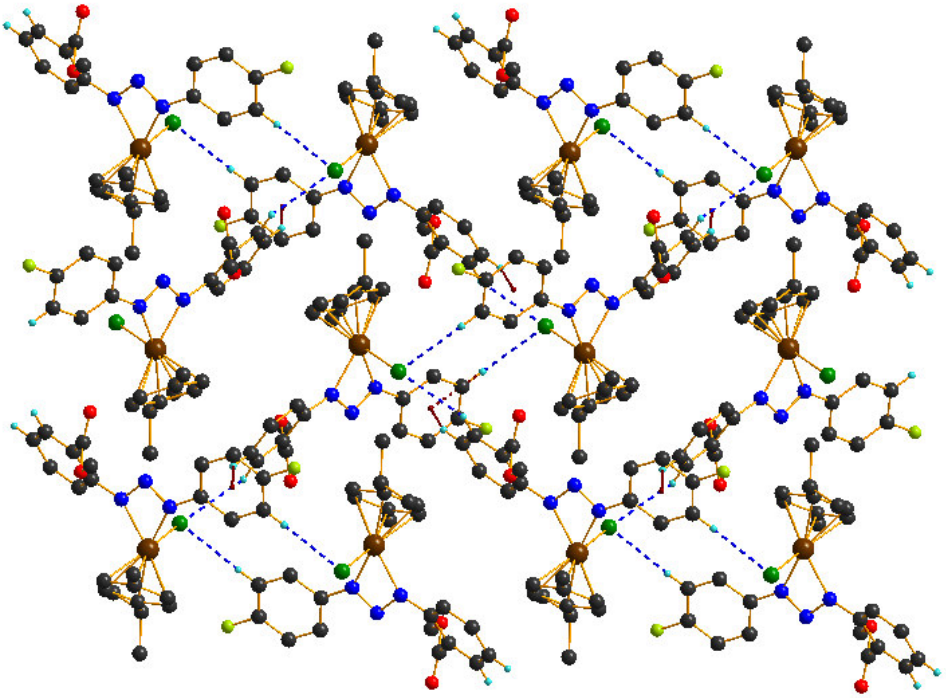

Figure 10. Representation of the 2D arrangement in complex **6**. Only the hydrogen atoms involved in the non covalent interactions have been drawn.

3.3. Transfer hydrogenation catalysis

To investigate the effects of the presence of different *para*-substituted triazenide ligands on the reactivity, complexes **6-10** were tested for their ability to catalyze the reduction of acetophenone to 1-phenylethanol under the conditions shown in Eq. (2).

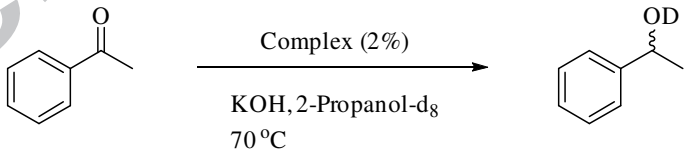

(2)

Table 2. Transfer hydrogenation of acetophenone using **6-10** as pre-catalysts.[a]

Entry	Pre-cat.	S/Cat/KOH	Time (h)	Yield (%)[b]
1	**6**	100:2:0	24	65
2	**7**	100:2:0	24	60
3	**8**	100:2:0	24	45
4	**9**	100:2:0	24	42
5	**10**	100:2:0	24	48
6	**6**	100:2:10	12	94
7	**7**	100:2:10	12	92
8	**8**	100:2:10	12	89
9	**9**	100:2:10	12	86
10	**10**	100:2:10	12	92

[a] Reaction conditions: 2-propanol-d_8, 70 °C, with or without KOH as base. [b]Yields were determined by ^{1}H NMR.

The results of the catalytic evaluation in the absence or in the presence of base are summarized in Table 2. Among pre-catalysts **6-9** with different *p*-halogen substituents, **6** with the *p*-F substituent in the 1,3-bis(aryl)triazenide ligand shows the best activity of transfer hydrogenation under base-free conditions, with a yield of 65% after 24 h of reaction (entry 1), whereas, **7** (*p*-Cl), **8** (*p*-Br) and **9** (*p*-I) show yields of 60, 45, and 42%, respectively (entries 2-4). These results indicate that the presence of a more electronegative *p*-halogen substituent in the 1,3-bis(aryl)triazenide ligand enhance the activity of the catalyst. This trend contrasts with O'connor's [(pyridinesulfonamide)Ir(Cp*)] catalyst system in which the transfer hydrogenation reactivity decreases with electron-withdrawing groups on the ligand [24]. Interestingly, pre-catalyst **10** (*p*-CH_3) is slightly more active than **8** (*p*-Br) and **9** (*p*-I), with a yield of 48% (entry 5) under the same conditions. This result was unexpected since the *p*-CH_3 group is less electronegative (a σ donor). However, it is difficult to compare the electronic effects between *p*-CH_3 and the *p*-halogen substituents since the halogens are σ acceptors and also π donors [43]. As can be observed in Fig. 11, no induction period was detected in any case, since production of 1-phenylethanol begins to form immediately after thermal equilibration of the reactant mixture.

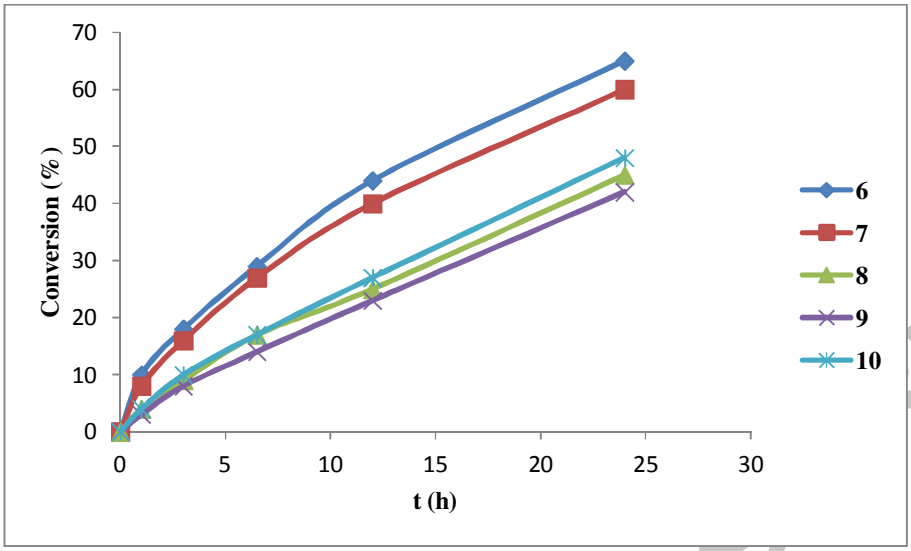

Figure 11. Reaction profile of conversion *vs* time for the catalytic transfer hydrogenation of acetophenone under base-free conditions, monitored by ^{1}H NMR.

When an external base is used, higher yields are obtained in shorter times, and the difference in reactivity between pre-catalyst decreases. For example, with the fastest pre-catalyst **6** and the slowest pre-catalyst **9**, conversions of 94 and 86%, respectively, are achieved after 12 h of reaction (Fig. S6).

Interestingly, the conversion obtained with pre-catalyst **6** in the presence of base is exactly the same than the conversion previously reported with pre-catalyst **A** (Fig. 2) under the same conditions (94% in 12 h) [21]. In contrast, when no external base is used the activity between **6** and **A** changed drastically, since a higher yield was obtained with **A** under the same conditions (65 *vs* 86%, respectively, in 24 h) [21]. It seems that under base-free conditions, the presence of a second *o*-methoxycarbonyl substituent in the triazenide ligand of **A** enhance the catalytic activity, probably by increasing the possibility of weak interactions between the hydride and the *ortho*-substituent with the substrate molecule [61]. Additionally, increasing the steric bulk of the ligand [22,23], probably brings the -$COOCH_3$ group close to the external coordination sphere of the ruthenium center more effectively [61]. Further studies would be needed to explain the role of the *ortho*- and *para*-substituents in the catalysis. However, experimental and computational studies by Jiménez et. al. showed that for Ir(I) carbene transfer

hydrogenation catalysts the presence of a pendant oxygen donor group enhance the catalytic activity through O···H interactions rather than oxygen to metal coordination [61].

Table 3. Transfer hydrogenation of acetophenone using **6** as pre-catalysts with different changes in the reaction media.[a]

Entry	Additive	Additive/cat. ratio	S/Cat/KOH	Time (h)	Yield (%)[b]
1	*p*-cymene	40/1	100:2:10	12	95
2	*p*-cymene	40/1	100:2:0	24	66
3	Hg	300/1	100:2:10	12	89
4	Hg	300/1	100:2:0	24	61
5	HCl	1/1	100:2:0	24	1%

[a] Reaction conditions: 2-propanol, 70 °C, with or without KOH as base. [b]Yields were determined by GC-MS.

Additional experiments were carried out with complex **6** as pre-catalyst in order to obtain information on the mechanism operating in the absence of base. First, a mercury poisoning experiment was conducted to test for heterogeneous catalysis (Table 3, entry 4). There was no significant impact on conversion from the addition of Hg(0); thus it is unlikely that heterogeneous sources of Ru are responsible for the activity observed [62].

Since one of the possible activation pathways could be decoordination of the *p*-cymene, an experiment in which free *p*-cymene was added to the reaction medium was run (Table 3, entry 2). The fact that an inhibition of the catalytic activity did not occur, indicates that decoordination of the arene does not occur during the catalytic process [22].

The same conclusions with the mercury poisoning experiment and the addition of free *p*-cymene have been obtained for the reaction in the presence of base (Table 3, entries 3 and 1, respectively).

Finally, the formation of hydrides in the absence or in the presence of base in 2-propanol was explored. First, pre-catalyst **6** in 2-propanol was heated at 70 °C in the presence of base. After 10 min of reaction the solvent was evaporated and a ^{1}H NMR spectrum in dry C_6D_6 was recorded. A hydride signal was detected at −12.52 ppm. In contrast, in the absence of base, after 6 h of reaction and treated in the same manner, the ^{1}H NMR spectrum showed two different hydride signals at −8.79 and −10.77 ppm. It is also noteworthy that a broad resonance

at low field (12.88 ppm), which can be ascribed to an NH group of the ligand, is also observed (free triazene **1** is not present in the reaction mixture).

These differences of activity in the presence or in the absence of base point to different reaction mechanisms for base-free and base-assisted catalysis. In the presence of base an inner-sphere mechanism is proposed [63]. On the other hand, based on what was found in the recent literature for transfer hydrogenation reactions under base-free conditions [25], an outer-sphere mechanism as shown in Scheme S1 (see Supporting information), in which one of the triazenide nitrogens acts as a base, is proposed. Theoretical calculations can be employed to her investigate mechanistic details. However, this is beyond the scope of

4. Conclusions

A series of four new triazenes of the type 1-[2'-(methoxycarbonyl)phenyl]-3-[4'-X-phenyl]triazene (X = F, Cl, Br, I) as precursors of triazenide ligands have been synthesized and characterized by IR, NMR and MS, and molecular structures determined by X-ray diffraction studies. Their corresponding ruthenium(II) complexes of formulae [Ru{1-(2'-methoxycarbonylphenyl)-3-(4'-X-phenyl)triazenide}(Cl)(*p*-cymene)] (X = F, Cl, Br, I, CH_3) were subsequently prepared and fully characterized by IR, NMR and HRMS. X-ray crystal structures of complexes **6** (X = F), **9** (X = I) and **10** (X = CH_3) were determined, which show common features with other Ru^{II}(*p*-cymene)triazenide complexes. Compounds **6**-**10** were tested in the catalytic reduction of acetophenone to 1-phenylethanol, either in the presence or the absence of a base. The best results were obtained in the presence of base with yields in the range of 86-94 %, whereas in the absence of base lower yields in the range 42-65% were achieved. This points to different reaction mechanisms: in the absence of base, an outer-sphere mechanism has been proposed [25], whereas in the presence of base an inner-sphere mechanism is proposed [63]. It is important to notice that although the yields are moderate in the absence of base, it is a good result since most pre-catalysts require a base to form the hydride complex as the active catalyst [26-30]. As hypothesized complexes **6-9** are active catalysts in the transfer hydrogenation of acetophenone. Their efficiency is dependent on the *p*-substituent with the *p*-F substituted being the most active in both base-free and base-assisted hydrogenations.

Acknowledgements

This work was supported by Consejo Nacional de Ciencia y Tecnología (CONACyT) Grant 60467 and Dirección General de Educación Tecnológica (DGEST) Grant 5150.13-P. E.C.-A and C.C.-A thank CONACyT for graduate fellowship. We thank CONACyT for ITT NMR and HRMS facilities (Grants INFR-2011-3-173395 and INFR-2012-01-187686). E.C.-A. thanks ESET, LLC for complementary financial support.

Appendix A. Supplementary material

CCDC 1538510 (**1**), 1541365 (**2**), 1538512 (**3**), 138513 (**4**), 138514 (**6**), 138515 (**9**), 138511 (**10**) contains the supplementary crystallographic data for this paper. These data can be obtained free of charge from The Cambridge Crystallographic Data Centre via www.ccdc.cam.ac.uk/data_request/cif.

Supplementary data associated with this article can be found, in the online version, at http://xxxxxxxxxxx

References

[1] K. Vrieze, G. Van Koten, Comprehensive Coordination Chemistry, vol. 2, Pergamon Press, Oxford, UK, 1987.

[2] D.B. Kimball, M.M. Haley, Angew. Chem., Int. Ed. 41 (2002) 3338-3351.

[3] D.V. Back, M. Hörner, F. Broch, G.M. Oliveira, Polyhedron 31 (2012) 558-564.

[4] A.P. Härter-Vaniel, A.E. Mauro, A.V.G. Netto, E. Tonon de Almeida, P.C. Piquini, P. Zambiazi, D.F. Back, M.J. Hörner, J. Mol. Struct. 1083 (2015) 311-318.

[5] T.V. Serebryanskaya, L.S. Ivashkevich, A.S. Lyakhov, P.N. Gaponic, Polyhedron 29 (2010) 2844-2850.

[6] L.Z. Fu, L.L. Zhou, S.Z. Zhan, Catal. Commun. 20 (2015) 26-29.

[7] M.F. Ibárra-Vázquez, S.A. Cortes-Llamas, A.A. Peregrina-Lucano, J.G. Alvarado-Rodriguez, R. Marríquez-González, F.A. López-Dellamary, M.I. Moreno-Brambila, I.I. Rangel-Salas, Inorg. Chim. Acta 451 (2016) 209-215.

[8] A. Hinz, A. Schulz, A. Villinger, J.M. Wolter, J. Am. Chem. Soc. 137 (2015) 3975-3980.

[9] M.C. Barral, R. Gonzáles-Prieto, S. Herrero, L.J. Priego, E.C. Royer, M.R.Torres, F.A. Urbanos, J.A. Reyes, Polyhedron 23 (2004) 2637-2644.

[10] S. Ibañez, L. Oresmaa, F. Estevan, P. Hirva, M. Sanaú, M.A. Úbeda, Organometallics 33 (2014) 5378-5391.

[11] P. Gantzel, P.J. Walsh, Inorg. Chem. 37 (1998) 3450-3451.

[12] H.S. Lee, S.O. Hauber, D. Vindus, M. Niemeyer, Inorg. Chem. 47 (2008) 4401-4412.

[13] J.G. Rodríguez, M. Parra-Hake, G. Aguirre, F. Ortega, P.J. Walsh, Polyhedron 18 (1999) 3051-3055.

[14] G. Ríos-Moreno, G. Aguirre, M. Parra-Hake, P.J. Walsh, Polyhedron 22 (2003) 563-568.

[15] J.J. Nuricumbo-Escobar, C. Campos-Alvarado, G. Ríos-Moreno, D. Morales-Morales, P.J. Walsh, M. Parra-Hake, Inorg. Chem. 46 (2007) 6182-6189.

[16] C. Tejel, M.A. Ciriano, G. Ríos-Moreno, I.T. Dobrinovitch, F.J. LaHoz, L.A. Oro, M. Parra-Hake, Inorg. Chem. 43 (2004) 4719-4726.

[17] J.J. Nuricumbo-Escobar, C. Campos-Alvarado, F. Rocha-Alonso, G. Ríos-Moreno, D. Morales-Morales, H. Höpfl, M. Parra-Hake, Inorg. Chim. Acta 363 (2010) 1150-1156.

[18] J. Sträle, C.F. Barboza, S. Schwarz, M.G. Mestres, S.T. López, S. T. Z. Anorg. Allg. Chem. 630 (2004) 1919-1923.

[19] G. Albertin, S. Antoniutti, J. Castro, S. Paganelli, J. Organomet. Chem. 685 (2010) 2142-2152.

[20] J. Košmrlj, M. Osmak, D. Urankar, I. Piantanida, M. Matković, A. Ambriović-Ristov, A. Pevec, A. Brozovic, I. Steiner, J. Vajs, J. Inorg. Biochem. 153 (2015) 42-48.

[21] E. Correa-Ayala, A. Valle-Delgado, G. Ríos-Moreno, D. Chávez, D. Morales-Morales, S. Hernández-Ortega, J.J. García, M. Flores-Álamo, V. Miranda-Soto, M. Parra-Hake, Inorg. Chim. Acta 446 (2016) 161-168.

[22] M.C. Carrión, F. Sepúlveda, F.A. Jalón, B.R. Manzano, Organometallics (2009), 28, 3822-3833.

[23] M. Kumar, J. DePasquale, N.J. White, M. Zeller, E.T. Papish, Organometallics 32 (2013) 2135-2144.

[24] A. Ruff, C. Kirby, B.C. Chan, A.R. O'Connor, Organometallics 35 (2016) 327-335.

[25] M.G. Sommer, S. Marinova, M.J. Krafft, D. Urankar, D. Schweinfurth, M. Bubrin, J. Košmrlj, B. Sarkar, Organometallics 35 (2016) 2840-2849.

[26] T. Ohkuma, M. Koizumi, K. Muniz, G. Hilt, C. Kabuto, R. Noyori, J. Am. Chem. Soc. 124 (2002) 6508-6509.

[27] K. Abdur-Rashid, S.E. Clapham, A. Hadzovic, J.N. Harvey, A.J. Lough, R.H. Morris, J. Am. Chem. Soc. 124 (2002) 15104-15118.

[28] Z.R. Dong, Y.Y. Li, J.S. Chen, B.Z. Li, Y. Xing, J.X. Gao, Org. Lett. 7 (2005) 1043-1045.

[29] M.A. Esteruelas, C. García-Yebra, E. Oñate, Organometallics 27 (2008) 3029-3036.

[30] V. Cadierno, P. Crochet, J. Díez, S.E. García-Garrido, J. Gimeno, Organometallics 23 (2004) 4836-4845.

[31] R. Corberán, E. Peris, Organometallics 27 (2008) 1954-1958.

[32] R. Castarlenas, M.A. Esteruelas, E. Oñate, Organometallics 27 (2008) 3240-3247.

[33] A. Picot, H. Dyer, A. Buchard, A. Auffarant, L. Vendier, P. Le Floch, S. Sabo-Etienne. Inorg. Chem. 49 (2010) 1310-1312.

[34] M.A. Bennett, T.N. Huang, T.W. Matheson, A.K. Smith, Inorg. Synth. 21 (1982) 74-75.

[35] *CrysAlis PRO* and *CrysAlis RED*. Agilent Technologies, Yarnton, **2013**.

[36] R.C. Clark, J.S. Reid, Acta Crystallogr., Sect. A: Found. Crystallogr. 51 (1995) 887.

[37] G.M. Sheldrick, Acta Crystallogr., Sect. A: Found. Crystallogr. 64 (2008) 112–122.

[38] L. Farrugia, J. Appl. Crystallogr. 30 (1997) 565.

[39] L. Farrugia, J. Appl. Crystallogr. 32 (1999) 837-838.

[40] G.M. Sheldrick, Acta Crystallogr., Sect. C: Struct. Chem. C71 (2015) 3-8.

[41] W.W. Hartman, J.B. Dickey, Org. Synth. 2 (1943) 163–165.

[42] M.K. Rofouei, M. Kamaee, S. Ramalingam, S.M. Sharifkhani, E. Fereyduni, Spectrochimica Acta Part A 90 (2012) 193-201.

[43] M. P. Rančić, N. P. Trišović, M. K. Milčić, I. A. Ajaj, A. D. Marinković, J. Mol. Struct. 1049 (2013) 59-68.

[44] M.P. Springer, C. Curran, Inorg. Chem. 2(1963) 1270–1275.

[45] P. Kapoor, A. Pathak, R. Kapoor, P. Venugopalan, Inorg. Chem. 41(2002) 6153-6170.

[46] A. Huczynski, J. Janczak, B.J. Brzezinski, Molec. Struct. 1030 (2012) 131–137.

[47] R. García-Álvarez, F.J. Suárez, J. Díez, P. Crochet, V. Cadierno, A. Antiñolo, R. Fernández-Galán, F. Carrillo-Hermosilla, Organometallics 31 (2012) 8301-8311.

[48] L. Menéndez-Rodríguez, E. Tomás-Mendivil, J. Francos, P. Crochet, V. Cadierno, A. Antiñolo, R. Fernández-Galán, F. Carrillo-Hermosilla, Organometallics 34 (2015) 2796-2809.

[49] T. Tsolis, M.J. Manos, S. Karkabounas, I. Zelovitis, A. Garaufis, J. Organomet. Chem. 768 (2014) 1-9.

[50] V. Cadierno, J. Díez, J. García-Álvarez, J. Gimeno, Organometallics 27 (2008) 1809–1822.

[51] V. Cadierno, J. Díez, J. García-Álvarez, J. Gimeno, Organometallics 23 (2004) 2421-2433.

[52]. M.R. Melardi, H.R.K. Ghaydar, M. Barkhi, M.K. Rofouei, Anal. Sci. 24 (2008) 281-282.

[53] M.K. Rofouei, M.R. Melari, Y. Salemi, J.A. Gharamaleki, Acta Crystallogr. E65 (2009) o2391.

[54] J.A. Charamaleki, M.R. Melardi, S.M. Hosseini, F. Hosseinzadeh, M. Peyman, M.K. Rofouei, Polyhedron 44 (2012) 138–142.

[55] M.R. Melardi, A. Ghannadan, M. Peyman, G. Bruno, H. Amiri, Acta Crysallogr. E67 (2011) o3485.

[56] F. Rocha-Alonzo, G. Aguirre, M. Parra-Hake, Acta Crystallogr. E65 (2009) o990-o991.

[57] Z. Ghalamic, J.A. Charamaleki, V. Ghoulipour, G. Bruno, H.A. Rudbari, M.K. Rofouei, Z. Anorg. Allg. Chem. 638 (2012) 798-803.

[58] R. Anulewicz, Acta Cryst. C53 (1997) 345-346.

[59] J.A. Charamaleki, A. Goodarzi, H. S. Bolouhari, S. Hooshmand, M.K. Rofouei, B. Notash, J. Inorg. Organomet. Polym. 25 (2015) 892-905.

[60] V. Ghoulipour, F. Hosseinzadeh, S. Farazi, J.A. Charamaleki, B. Notash, M.K. Rofouei, J. Coord. Chem. 67 (2014) 2171-2183.

[61] M.V. Jiménez, J. Fernández-Tornos, J.J, Pérez-Torrez, F.J. Modrego, S. Winterle, C. Cunchillos, F.J. Lahoz, L.A. Oro, Organometallics 30 (2011) 5493-5508.

[62] D.R. Anton, R.H. Crabtree, Organometallics 2 (1983) 855-859.

[63] S.E. Clapham, A. Hadzovic, R.H. Morris, Coord. Chem. Rev. 248 (2004) 2201-2237.

Graphical abstract

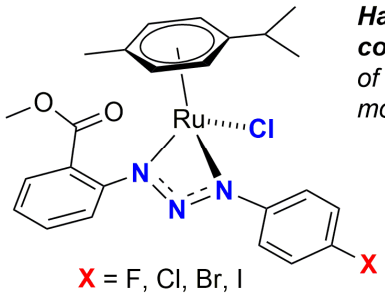

Halogen p-substituted triazenide ligands in Ru(II) complexes *are active catalysts in the transfer hydrogenation of acetophenone with good yields (86-94% with base) and moderate yields (42-65% without base).*

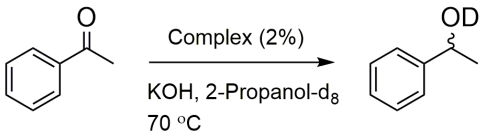

Highlights

- Ruthenium triazenide complexes as catalysts for hydrogenation of ketones.
- Crystal structures of triazene precursors and Ru^{II}(*p*-cymene) complexes.
- Base assisted and base free hydrogenation by ruthenium triazenide complexes.